JOURNAL OF MATERIALS SCIENCE 28 (1993) 1551–1556

Surface treatment of a 316L type stainless steel by explosive: microstructural characterization and monotonic tensile behaviour

M. GERLAND, H. N. PRESLES*, J. MENDEZ, J. P. DUFOUR
*Laboratoire de Mécanique et Physique des Matériaux, URA CNRS 863, and *Laboratoire d'Energétique et Détonique, URA CNRS 193, ENSMA, 86034 Poitiers, France*

A new surface-treatment process using a thin layer of primary explosive was applied to a 316L type stainless steel. The induced microstructural modifications and the residual mechanical properties of the treated material have been evaluated. The surface roughness quality and the microhardness increase are higher than after usual shot-peening treatments. The near-surface microstructure, observed by transmission electron microscopy, is composed of numerous mechanical twins the density of which decreases with increasing depth. The yield strength (0.2% offset) of the treated layer has been evaluated and related to the mean value of the microhardness in this layer.

1. Introduction

The most commonly used methods to increase surface hardness in order to improve wear, corrosion or fatigue resistance of materials can be classified into three main categories:

(i) thermal processes producing a superficial quenching (blowlamp heating, electron beams or high power continuous laser, etc.);

(ii) thermochemical processes (nitridation, carburation, plasma deposition, etc.);

(iii) cold mechanical strengthening processes (shot peening, wheeling, flyer plate impact of laser induced shock waves, etc.).

The use of explosives for material surface treatment enables the strengthening effects due to shock waves and the thermal effects due to the high temperature of the detonation products to be combined. Treatments of structures such as rails or excavation material have already been performed using secondary-type explosives supplying very high pressures (some tens of giga pascals). These explosives are not very sensitive and need amplitude shock waves of some giga pascals to be brought into detonation. However, the high-amplitude shock waves generated by secondary explosives can produce detrimental effects and damage in the treated surfaces. On the other hand, primary explosives are less powerful but essentially dangerous to handle and the utmost care must be exercised in all dealings with them. Their sensitiveness is such that they can easily be brought into detonation by a slight shock or any flame or spark; however, their high sensitivity gives them the property to detonate in very thin layers. The critical thickness of these explosives (the thickness below which the detonation cannot propagate) is markedly lower than 1 mm, even if unconfined. In the same conditions, this thickness reaches several millimetres with secondary explosives and several centimetres with industrial explosives. So, with their moderate characteristics of detonation and their low critical thickness, primary explosives could be expected to be used with success for surface treatments of materials. A new technique using primary explosive has been used here to treat a stainless steel: after having characterized induced microstructural modifications on the near surface layer, residual mechanical properties of the treated material have been evaluated.

2. Experimental procedure

2.1. Material

The studied material was an austenitic stainless steel type AISI 316L (AFNOR Z3 CND 17-12 named ICL 167 SPH) whose composition and mechanical characteristics are given in Tables I and II, respectively.

All the specimens used for microstructural studies or for tensile tests were first polished, then heat treated for 1 h at 1050 °C in high vacuum (about 5×10^{-4} Pa) and water cooled; they were then polished again up to 1 μm diamond to remove the oxyde layer. The mean grain size was about 50 μm.

2.2. The surface-treatment technique

The explosive product used for surface treatment was prepared in our laboratory (URA CNRS 193) by mixing a primary explosive and a liquid inert binder. The explosive substance was applied like a paint with a brush on the whole surface chosen to be treated. The detonation was initiated in the periphery by a laser pulse, and then spread over the whole area concerned. Different thicknesses of the explosive layer varying

0022–2461

TABLE I Chemical composition (wt %) of ICL 167 SPH stainless steel

	Element												
	C	Mn	Si	S	P	Ni	Cr	Mo	Cu	B	N_2	Co	As
Amount (wt %)	0.022	1.69	0.31	0.002	0.023	11.90	17.45	2.25	0.110	0.009	0.069	0.190	0.004

TABLE II Mechanical characteristics of ICL 167 SPH stainless steel at 20 °C.

Yield strength; Y (MPa)	Ultimate tensile Strength, S_u (MPa)	Elongation, e (%)
254	583	53

from 0.3–1 mm have been tested. After the explosion, the treated surfaces are partially covered with detonation products. These adherent residues are eliminated by a cleaning of the surfaces by ultrasonics followed by a stripping during 30 s at 20 °C in a solution composed of 10 g ferric chloride, 30 cm^3 hydrochloric acid and 250 cm^3 H_2O during 30 s at 20 °C.

2.3. Characterization of the effects induced by the treatment

The effects induced in the material by the surface treatment were investigated by different means: evaluation of the surface topography using a Talisurf profile apparatus; microhardness profiles measurements with a load of 25 g in two different ways (on a section normal to the treated surface, or on the surface, starting from the treated surface and removing successive parallel layers by mechanical polishing); microstructural studies by transmission electron microscopy (TEM) under 100 kV on thin foils taken at different depths from the treated surface.

2.4. Tensile specimens

As the surface treatment affects a very thin layer of matter, it was not possible to machine a specimen thin enough to be treated as a whole without buckling. Therefore, tensile tests were always performed on specimens with thicknesses always greater than 1 mm and with different sections in order to obtain various proportions of the treated material in relation to the untreated material, the affected depth being the same for a given thickness of explosive.

The tensile tests were performed (a) on specimens with a rectangular section (6 mm × 1 mm or 6 mm × 4 mm) and a gauge length of 38 mm. These specimens were treated with an explosive thickness of 0.5 or 0.6 mm, or (b) on cylindrical specimens with a diameter of 4 or 6 mm and a gauge length of 20 mm. These specimens were treated with an explosive thickness of 0.9 or 1 mm.

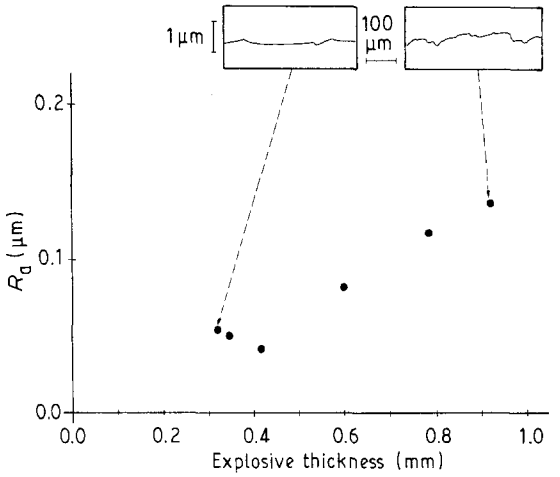

Figure 1 Roughness evolution of the treated surface as a function of explosive layer thickness.

Tensile tests were performed without stripping of the detonation products. They were performed at room temperature on an Instron machine with a crosspiece controlled rate of 5 mm min^{-1}.

3. Results

3.1. Surface topography

The surface topography was determined by the use of a Talisurf profile apparatus which allows evaluation of the undulation of the surface which characterizes the flatness defects and the roughness given by the arithmetic deviation to a mean line. No flatness defect was found whatever the sample. On the other hand, the roughness factor, R_a, near zero after polishing, remained very low even in the case of the most severe treatment conditions, because only an increase of 0.15 μm was found with an explosive layer 1 mm thick (Fig. 1).

3.2. Microhardness measurements

The microhardness profiles obtained by the two different methods (on a section normal to the treated surface or on planes parallel to the surface) are very similar; therefore only one example obtained on a normal section is given on Fig. 2 for the extreme conditions of treatment: 0.3 and 1 mm explosive thickness. Every point of the curves corresponds to the average value of 25 measurements of microhardness. Fig. 2 shows similar effects concerning the position of the hardness peak value situated at 20 and 30 μm beneath the surface, whatever the explosive thickness.

Only the intensity of the effects varies with the explosive thickness: with a thin layer of 0.3 mm, the hardness peak is weak and the treated depth is only about 100 μm; on the other hand, with a 1 mm thick layer, the hardness peak reaches 300 Hv instead of 180 Hv in the untreated material and the modified depth reaches 200 μm. The hardness decrease near the surface is supposed to be due to thermal effects because of the high temperature of the detonation products estimated to be about 3000 K.

3.3. TEM observations

Microstructural studies by TEM were performed on samples treated with an explosive thickness varying from 0.3–0.8 mm at different depths beneath the treated surface. The thinning method allows estimation of the depth at which the TEM observations are performed: for example a thin foil of 80 μm taken from the surface (in fact cut at 600 μm depth then mechanically thinned from the rear face) thinned by the double-jet technique will give thin areas situated at around 40 μm in depth. In order to obtain thin areas at 80 μm in depth or at the surface, the rear face or the front part is protected by a plastic film during all the thinning process. In order to obtain observation areas at intermediate depths, the plastic film is removed during the process of thinning.

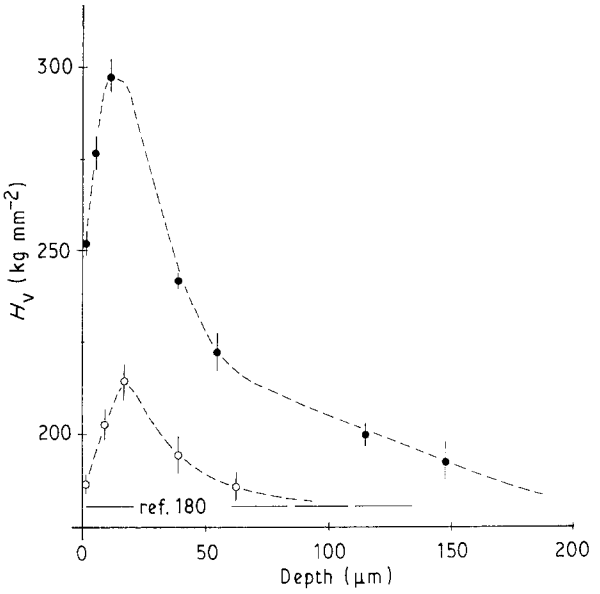

Figure 2 Microhardness profiles on samples treated with explosive layer thickness of (○) 0.3 and (●) 1 mm.

Whatever the explosive thickness, the near surface microstructure is composed of numerous mechanical twins the density of which decreases when depth increases. For small explosive thicknesses (0.3–0.4 mm) the high twin density layer is present from the surface up to 20 μm in depth, with two or three twin sets in most of the grains and a mean spacing of 0.2 μm. Beneath this surface layer, up to 50 μm in depth, the microstructure is composed of some twins with a mean spacing of 1 μm and dislocation tangles in a low density. For high explosive thicknesses (0.6–0.8 mm) the same microstructures are observed but the affected depths are higher, respectively 40 μm for the high twin density layer and 80 μm for the layer consisting of a mixture of twins, tangles and some walls (Figs 3 and 4). At higher depths, only dislocations with higher density than in the untreated material are seen up to 100 μm for small explosive thicknesses and up to 150 μm for high explosive thicknesses.

3.4. Tensile tests

The results of tensile tests (yield strength (0.2% offset), Y; ultimate tensile strength; S_u, elongation, (e) are gathered in Table III.

The volumic treated fraction, f_T, corresponds to the ratio S_T/S, where S_T is the treated area on a specimen section and S the total area of this section. The treated surface is calculated by taking the treated depth, d, equal to the value corresponding to the maximal depth at which an increase in the microhardness is observed; d is close to 100 μm for an explosive thickness of 0.5 mm and to 200 μm for an explosive thickness of 1 mm. Under these conditions, the expressions

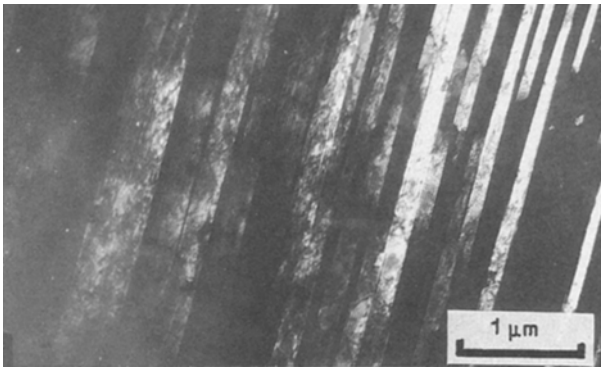

Figure 3 Dark-field transmission electron micrograph of a sample treated with an 0.6 mm explosive thickness at a depth of 20 μm, showing mechanical twinning with a mean twin spacing of 0.2 μm.

TABLE III Mechanical characteristics of treated specimens as a function of treatment conditions

Section shape	Explosive thickness (mm)	Section sizes (mm)	True surface (mm^2)	Y (MPa)	S_u (MPa)	e (%)	$f_T = \frac{S_T}{S}$ (%)
Rectangular	0.5	6 × 4	24	285	587	53	8
Rectangular	0.5	6 × 1	6	335	570	57	23
Circular	1	6	28.3	325	–	–	13
Circular	1	4	12.5	380	622	44	20

Figure 4 Bright-field transmission electron micrograph of a sample treated with an 0.6 mm explosive thickness at a depth of 40 µm, showing dislocation walls in addition to mechanical twinning.

for the treated surface are given by

$$f_T = \frac{2d(w + t)}{wt} \quad (1)$$

where w is the sample width, t the sample thickness, and d the treated depth, for samples with a rectangular section and by neglecting the d^2 terms, and

$$f_T = \frac{2d}{r} \quad (2)$$

where r is the sample radius, and d the treated depth, for samples with a circular section and by neglecting the d^2 terms.

The yield strength (0.2% offset) of the treated samples is higher than the yield strength of the untreated material (254 MPa) and roughly increases with the volumic treated fraction, f_T. The ultimate tensile strength, S_u, and the elongation, e, do not vary very much, the treated fraction remaining low. The elongation of the sample with a rectangular section (6 mm $\times$ 1 mm) cannot be directly compared with the other values because the low thickness of this sample has, as a consequence, reduction of area [1].

During the different tensile tests, no evolution of the elasticity modulus was observed; although the tensile test is not precise enough to assert that there is no modification of the elasticity modulus induced by the treatment, we will admit that the Young modulus of the treated layer (E_T) and of the untreated material (E_U) are equal: $E_T = E_U = 198$ GPa.

4. Discussion

4.1. Evaluation of the mechanical characteristics of the treated layers

From the tensile curves of the untreated and treated samples, the yield strength (0.2% offset) of the treated layer alone can be evaluated. First it will be supposed that the treated layer is uniform and is 100 µm deep for the rectangular samples with a 0.5 mm thick explosive or 200 µm deep for the circular samples with a 1 mm thick explosive. The values of 100 µm (or 200 µm) for the treated layer are deduced from the hardness curves obtained in a sample treated with a 0.5 mm (or 1 mm) thick explosive. Second, it will be supposed that beyond the treated layer of 100 µm (or 200 µm), the material is in the initial state, identical in every way to the untreated material.

In order to deform such a modellized sample to a total strain level ε_T, a tensile force, $\bar{F}$, has to be applied to it. This tensile force can be resolved into

$$\bar{F} = F_T + F_U \quad (3)$$

where F_T is the force necessary to deform the treated layer up to ε_T and F_U is the force necessary to deform the untreated part of the sample beneath the treated layer up to the same ε_T.

Equation 3 can be rewritten

$$\bar{\sigma}S = \sigma_T S_T + \sigma_U S_U \quad (4)$$

where $\bar{\sigma}$ (or σ_T, σ_U) is the strength corresponding to $\bar{F}$ (or F_T, F_U) in the total section S (or S_T (treated area), S_U (untreated area)), or

$$\bar{\sigma} = \sigma_T \frac{S_T}{S} + \sigma_U\left(1 - \frac{S_T}{S}\right) \quad (5)$$

where $\frac{S_T}{S}$ is the treated fraction f_T given by Equation 1 for a sample with a rectangular section and by Equation 2 for a sample with a circular section

Finally Equation 5 can be rewritten

$$\sigma_T = \frac{\bar{\sigma} - \sigma_U(1 - f_T)}{f_T} \quad (6)$$

This last relation enables us to build point by point the tensile curve of the entirely treated material from the tensile curves corresponding to the untreated and treated samples. For example, Fig. 5 gives the tensile curves of the untreated material and of the sample with a rectangular section (6 mm $\times$ 1 mm) treated with a 0.5 mm thick explosive. For every thousandth of the total deformation ($\varepsilon_T = 10^{-3}$, $\varepsilon_T = 2 \times 10^{-3}$, $\varepsilon_T = 3 \times 10^{-3}, \ldots$) between $\varepsilon_T = 0$ and 10^{-2}, Equation 6 can be applied by noting the σ_U value on the tensile curve of the untreated material and the $\bar{\sigma}$ value on the tensile curve of the treated sample; f_T, calculated from Equation (1), is given in Table III. This method allows us to construct graphically the tensile curve of the fully treated material with an explosive thickness of 0.5 mm. From the test on the 6 mm $\times$ 1 mm specimen, the yield strength (0.2% offset) of the fully treated material is about 600 MPa. With the same method, the yield strength (0.2% offset) of the treated layer of the sample with a rectangular section (6 mm $\times$ 4 mm) is very similar being estimated to be 575 MPa. Therefore, the treated layer with a 0.5 mm thick explosive has a yield strength (0.2% offset) close to 600 MPa, that is more than twice as high as the yield strength of the untreated material (254 MPa, see Table II). Another example is given by Fig. 6 showing the tensile curves of the untreated material and of the sample with a circular section (6 mm diameter) treated with an explosive thickness of 1 mm. The same process of graphic construction point by point gives the tensile curve of the fully treated material with an explosive thickness of 1 mm. In this case the yield strength (0.2%

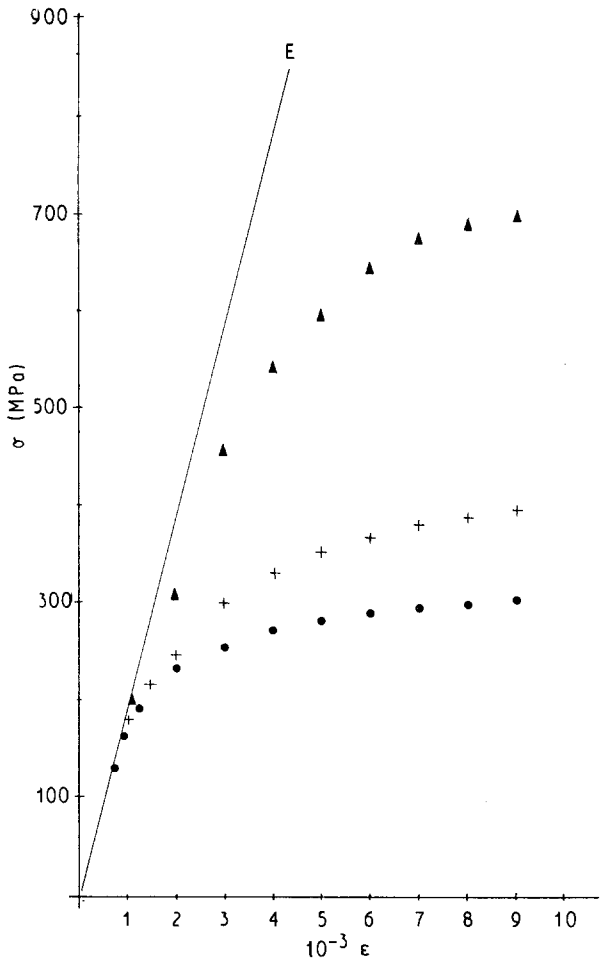

Figure 5 Experimental tensile curves of (●) the untreated material and of (+) the sample (rectangular section 6 mm × 1 mm) treated with a 0.5 mm thick explosive. (▲) Graphic construction of the tensile curve of the fully treated material with a 0.5 mm thick explosive.

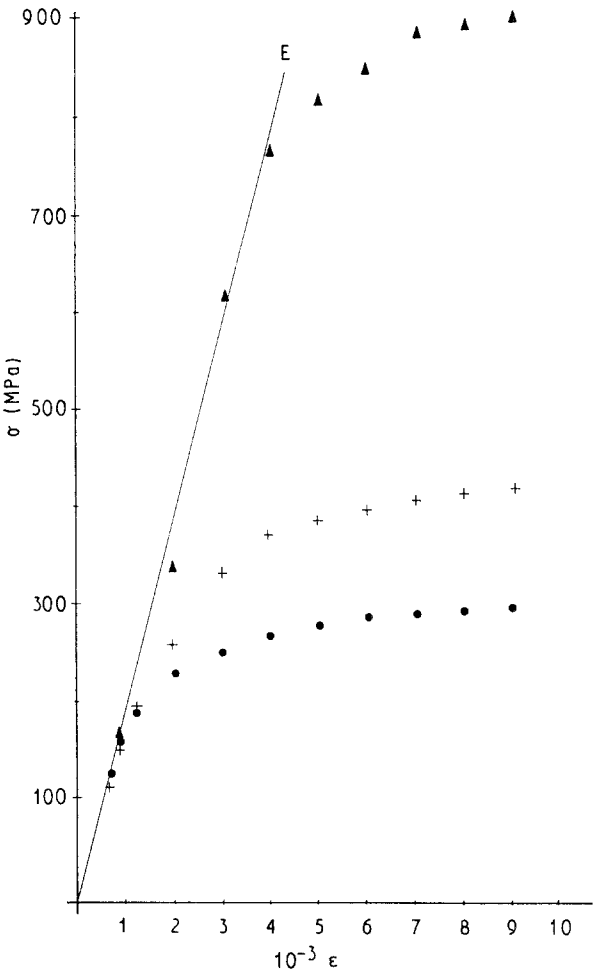

Figure 6 Experimental tensile curves of (●) the untreated material and of (+) the sample (circular section 4 mm diameter) treated with a 1 mm thick explosive. (▲) Graphic construction of the tensile curve of the fully treated material with a 1 mm thick explosive.

offset) reaches 850 MPa, that is markedly higher than that of the material treated with an explosive thickness of 0.5 mm. The increase of the yield strength with the explosive treatment can be related to the increase of hardness in the treated layer by the empirical relation

$$H_T = A \ln Y_T \quad (7)$$

where H_T is the mean microhardness value on the whole treated layer, i.e. 100 μm (or 200 μm) for a 0.5 mm (or 1 mm) thick explosive, Y_T is the yield strength (0.2% offset) of the fully treated material with 0.5 mm (or 1 mm) thick explosive, and A is a constant. H_T was estimated to be 200 Hv (or 215 Hv) for the material treated with an explosive thickness of 0.5 mm (or 1 mm); for the untreated material, the reference microhardness is 180 Hv and the yield strength is 254 MPa. With these conditions the constant A in Equation 7 is very close to 32.

4.2 Relation between microhardness and microstructure

The hardness increase in the treated layers is related to the high twin density, and the lower values of microhardness in the first 20 μm is supposed to be due to annealing effects because of the high temperature of the detonation products. Although insufficient observations in TEM are available due to the difficulty of realizing thin foils in very strengthened layers, the microhardness decrease with depth in the treated material can be associated with the twin and dislocation density decrease. However, a direct correlation point by point between the hardness curves and the evolution of the microstructure as a function of the depth cannot be made. Contrary to what was noted on the same material in similar investigations of laser-treatment effects [2,3], no marked difference in the twin density with the explosive thickness was noted, as could be expected from the difference in the microhardness peak values (see Fig. 2).

4.3. Comparison of the explosive treatment with other surface-treatment techniques

The effects induced by the treatment by explosive used in this study appear interesting compared with those induced by other techniques such as shot peening and laser shock waves. The surface topography after the explosive treatment is very good, because R_a remains below 0.15 μm even for the most severe conditions of treatment with 1 mm explosive thickness (Fig. 1), contrary to what is observed in the case of a shot-peening

treatment. For example, Gentil *et al.* [4] have noted, on a shot-peened E460 steel, a 5 μm thick spalling or microcracks close to 10 μm in depth and a surface roughness of 7.5 μm for a 100% covering level. Wohlfahrt [5] has observed, for materials with a high hardness, an R_a factor of 2–3 μm and, for materials with a low hardness, a roughness of 13–25 μm. After a laser shock-wave treatment, the surface topography generally has a poor quality with formation of craters in focusing conditions [6], molten material ejections [7], or suddenly congealing concentric wave formation [8–10] in plane irradiation conditions. Furthermore, the area treated by means of laser shock, remains limited.

The depth hardened by the explosive treatment reaches 100–200 μm (Fig. 2), that is of the same order as by shot peening; however, the hardness increase reaches 70% in the stainless steel (Fig. 2) and 100% in copper [11] by the explosive treatment, while it generally does not exceed 50% by shot peening. On the other hand, the hardness increase is similar to that obtained by laser shock waves [12, 13] in spite of different shock characteristics in the two techniques: pulse duration of about 1 μs [14] for the explosive shock and of about 1 ns for the laser shock [12, 13], and maximum pressure of about 1–2 GPa for the explosive shock used in this study [14] and more than 10 GPa for the laser shock [2, 12, 13]. The decrease in the induced effects as a function of the depth is due to faster damping of the shock wave because the pulse is short.

The high mechanical characteristics of the treated layers associated with a very low roughness of the surface make study of the application of this technique to the improvement of the fatigue resistance of materials very interesting. Such a study, previously realized on polycrystalline copper [11], has subsequently been performed on the 316 L stainless steel and will be published elsewhere.

5. Conclusion

A new surface-treatment technique using primary explosive was performed on a 316 L type stainless steel. The effects induced in the material by the surface treatment as a function of the explosive thickness were investigated by different means, with the following characteristics.

1. The roughness factor, R_a, near zero before treatment, remains very low; even for an explosive thickness of 1 mm, R_a remains lower than 0.15 μm.

2. Microhardness profiles are characterized by a maximum peak situated at 20 or 30 μm beneath the surface whatever the explosive thickness, with a maximum value for 1 mm explosive thickness reaching 170% of the value for the untreated material. The treated depth is about of 100 μm with a 0.3 mm thick explosive and reaches 200 μm for an explosive thickness of 1 mm. The lower microhardness increase in the surface layers is attributed to thermal effects.

3. Whatever the explosive thickness, the microstructure is characterized near the surface by numerous mechanical twins, the density of which decreases as depth increases. Beneath the twinned area, a mixture of some twins, dislocation walls and tangles was observed with a decreasing density as depth increases. The extents of twins alone and of the mixture of twins and dislocations are, respectively, 20 and 30 μm for small explosive thicknesses (0.3–0.4 mm) and 40 μm in both cases for high explosive thicknesses (0.6–0.8 mm). Beneath the two previous layers, only dislocations are present up to the limit of the hardened zone with a density higher than in the untreated material.

4. The yield strength (0.2% offset) of the treated layer was estimated to be more than twice (or three times) the yield strength of the untreated material after surface treatment with 0.5 mm (or 1 mm) thick explosive. The mean microhardness, H_T, and the yield strength of the treated layer, Y_T, can be related by $H_T = A \ln Y_T$, where A is a constant.

Acknowledgements

The authors thank Professor J. P. Romain, URA CNRS 193, for help in conceiving the process and Dr J. Parisot, URA CNRS 863, for his help with the tensile tests.

References

1. M. GRUMBACH, "Propriétés d'emploi des aciers, l'essai de traction."(IRSID-OTUA, Paris 1976).
2. M. HALLOUIN, M. GERLAND, J. P. ROMAIN, L. MARTY and F. COTTET, *J. Phys. C3 Supp.* 19 **49** (1988) 413.
3. M. GERLAND and M. HALLOUIN, in "Surface Modification Technologies IV", edited by T. S. Sudarshan, D. G. Bhat and M. Jeandin (The Minerals, Metals and Materials Society, 1991) pp. 895–902.
4. B. GENTIL, M. DESVIGNES and L. CASTEX, *Matér. Techn.* December (1987) 493.
5. H. WOHLFAHRT, in "Proceedings of the 2nd International Conference on Shot Peening", Chicago, May 1984, pp 316–31.
6. M. HALLOUIN, M. GERLAND, F. COTTET, J. P. ROMAIN and L. MARTY, *Mem. Et. Sci. Rev. Metall.* **1** (1987) 25.
7. J. P. DUFOUR, M. GERLAND and P. DARQUEY, *Scripta Metall.* **23** (1989) 483.
8. S. ALTSHULIN, J. ZAHAVI, A. ROSEN and S. NADIV, *J. Mater Sci.* **25** (1990) 2259.
9. K. ROZNIAKOWSKI, *J. Mater. Sci. Lett.* **4** (1985) 790.
10. D. GREVEY, L. MAIFFREDY, A. B. VANNES and P. F. GOBIN, *Scripta Metall. Mater.* **24** (1990) 767.
11. M. GERLAND, J. P. DUFOUR, H. N. PRESLES, P. VIOLAN and J. MENDEZ, *J. Phys. III* **1** (1991) 1647.
12. M. GERLAND, M. HALLOUIN and H. N. PRESLES, *Mater. Sci. Eng.* **A156** (1992) 175–182.
13. M. GERLAND and M. HALLOUIN, *J. Mater. Sci.* submitted.
14. H. N. PRESLES, unpublished results (1990).

Received 15 October 1991
and accepted 4 August 1992